Quantum Localization of the Kicked Rydberg Atom

S. Yoshida,[1] C. O. Reinhold,[1,2] and J. Burgdörfer[1,2,3]

[1]*Department of Physics, University of Tennessee, Knoxville, Tennessee 37996-1200*
[2]*Physics Division, Oak Ridge National Laboratory, Oak Ridge, Tennessee 37831-6373*
[3]*Institute for Theoretical Physics, Vienna University of Technology, A1040 Vienna, Austria*

(Received 3 September 1999)

We investigate the quantum localization of the one-dimensional Rydberg atom subject to a unidirectional periodic train of impulses. For high frequencies of the train the classical system becomes chaotic and leads to fast ionization. By contrast, the quantum system is found to be remarkably stable. We find this quantum localization to be directly related to the existence of "scars" of the unstable periodic orbits of the system. The localization length is given by the energy excursion along the periodic orbits.

PACS numbers: 32.80.Rm, 03.65.Sq, 05.45.Mt, 42.50.Hz

Even though the correspondence between classical and quantum mechanics has been extensively investigated for nearly a century, many issues have remained unresolved. Renewed interest in this subject has recently been stimulated by the experimental realization of simple driven systems that are at the borderline between classical and quantum mechanics. Prototypes of such systems are cooled atoms subject to modulated standing waves [1], Rydberg atoms subject to microwave pulses [2], and Rydberg atoms subject to trains of half-cycle pulses [3,4].

One important motivation for revisiting the issue of classical-quantum correspondence has been the increased appreciation of the apparent contradiction between the ubiquitousness of classical chaotic dynamics and the lack thereof in quantum dynamics. This suggests that, even in the limit of large quantum numbers, the correspondence between classical and quantum dynamics cannot hold for arbitrary periods of time. One of the most interesting discoveries along these lines has been the quantum localization or quantum suppression of classically chaotic diffusion. Quantum localization was first predicted for the kicked rotor [5]. It was shown that quantum localization can be mapped onto the well-known Anderson localization in solid state physics [6,7]. Subsequently, it was found for Rydberg atoms in microwave fields [8,9] and could be observed as an enhanced quantum stabilization of the atom against ionization. Recently, quantum localization for these systems has been confirmed experimentally [1,2].

In this Letter we investigate the quantum localization in the "kicked Rydberg atom." Experimental realization of this driven system has only recently been achieved by exposing Rydberg atoms with $n_i \sim 400$ to trains of many equispaced half-cycle pulses [3,4]. This system can display both "hard" (global) and "soft" (coexisting with regular dynamics) chaos, depending on the direction, the strength, and the frequency of the train of kicks [3,4,10]. For pulse repetition frequencies ν_T close to the classical orbital frequency (i.e., $\nu_T^{-1} \simeq T_{\rm orb} = 2\pi n_i^3$, where n_i is the initial energy level and atomic units are used throughout), both classical and quantum calculations exhibit enhanced stability in good agreement with experiment which is a signature of broad stable islands in phase space [11]. For high frequencies ($\nu_T T_{\rm orb} \gg 1$), however, a drastically different picture emerges: the classical system is fully chaotic over a wide range of kick strengths and directions resulting in rapid ionization. Here we show that the quantum system exhibits strong suppression of classical chaotic ionization. Quantum localization is found to exhibit novel features different from previously studied systems. The strong impulsive coupling leads to localization in the continuum and to deviation from exponential localization. These features can be directly traced to scars of unstable periodic orbits.

Converged quantum calculations in three dimensions (3D) for the long-time evolution of systems with strong coupling to the continuum remain a challenge. We therefore focus here on a simplified one-dimensional (1D) system for which convergence can be achieved. The latter is crucial for the determination of long-time stability and localization. The 1D system is described by the Hamiltonian

$$H(t) = H_{\rm at} + V(t), \tag{1}$$

$$H_{\rm at} = \frac{p^2}{2} - \frac{1}{q}, \qquad V(t) = -q\Delta p \sum_{k=0}^{K-1} \delta(t - kT), \tag{2}$$

where $q > 0$ and p are the position and momentum of the electron, respectively, and $H_{\rm at}$ is the unperturbed atomic Hamiltonian. The train of δ-shaped kicks is characterized by the total number of kicks K, the kick strength Δp, and the time period between kicks T (i.e., the train frequency $\nu_T = 1/T$). The classical phase-space structure of this simplified model was found to closely mimic that of the 3D system for initial conditions representing elongated (Stark) orbits [4]. This similarity is partly due to the fact that the kicked atom features a global chaotic sea for arbitrarily small Δp (Fig. 1). The Poincaré surface of section for this time-dependent system corresponds to stroboscopic snapshots of the scaled $(q_0, p_0) = (q/n_i^2, pn_i)$ coordinates just before each kick (Fig. 1). No matter how small the value of Δp is, the classical phase space undergoes a discontinuous transition as the perturbation is turned on. For the "positively" kicked atom, $\Delta p > 0$, the system

 0031-9007/00/84(12)/2602(4)$15.00

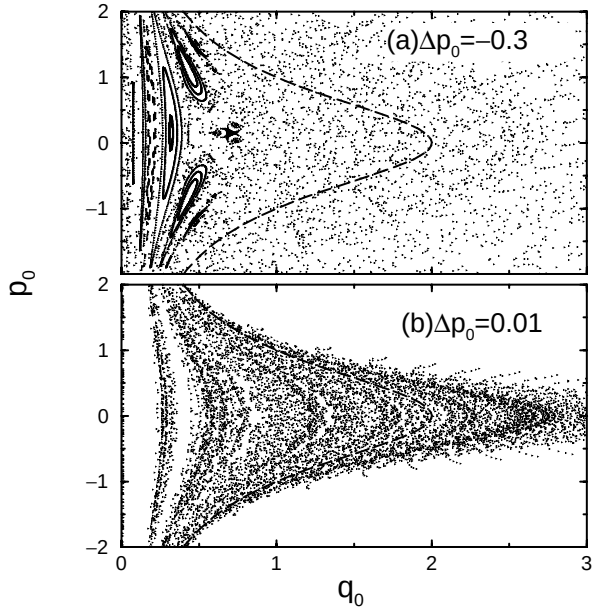

FIG. 1. Poincaré maps of the kicked atom (dots) together with the unperturbed torus associated with the initial state (dashed line) in scaled units, $q_0 = q/n_i^2$ and $p_0 = n_i p$. The frequency of the train of pulses is $\nu_0 = 16.8$.

immediately displays hard chaos: all tori are suddenly destroyed [Fig. 1(b)] [10]. For the "negatively" kicked atom, $\Delta p < 0$, the system suffers a transition to soft chaos with a mixed phase space. Residual tori are not globally confining and an interconnected chaotic sea permits diffusion to the continuum [Fig. 1(a)].

The strong coupling between bound states and the continuum distinguishes the kicked atom from other systems. The Fourier expansion of the interaction

$$V(t) = -\frac{q\Delta p}{T} - \frac{2q\Delta p}{T}\sum_{m=1}^{\infty}\cos(2\pi\nu_m t) \qquad (3)$$

contains all harmonics ($\nu_m = m\nu_T$) with equal strength leading to multiphoton coupling to the continuum. Unlike laser or microwave fields, the average field, $F_{\rm av} = -\Delta p/T$, is nonzero. Therefore, the Hamiltonian contains both static (dc) and dynamic (ac) electric fields,

$$\begin{aligned} H(t) &= H_{\rm Stark} + V'(t) = H_{\rm at} + qF_{\rm av} + V'(t)\,, \\ V'(t) &= 2qF_{\rm av}\sum_{m=1}^{\infty}\cos(2\pi\nu_m t)\,. \end{aligned} \qquad (4)$$

For $\Delta p < 0$ ($F_{\rm av} > 0$), the quantum spectrum of $H_{\rm Stark}$ is discrete. For $\Delta p > 0$ ($F_{\rm av} < 0$), the spectrum is entirely continuous and involves a finite number of resonances whose energy levels are below or near the top of the potential barrier $E_{\rm barrier} = -2\sqrt{\Delta p/T}$. Equivalently, the effect of the perturbation [Eq. (2)] corresponds to a sequence of energy transfers

$$\Delta E_k = \langle H_{\rm at}\rangle_{k+1} - \langle H_{\rm at}\rangle_k = \langle p\rangle_k \Delta p + \frac{\Delta p^2}{2}\,, \qquad (5)$$

showing that the momentum transfer, in addition to the frequency, determines the effective energy transfer.

The strong coupling to the continuum complicates the quantum description since any realistic calculation must include a large number of continuum states. Quantum calculations are performed by expanding the wave function of the electron, $|\psi(t)\rangle$, in a large basis set of Sturmian pseudostates (up to $N_{\rm max} = 1500$) spanning a finite Hilbert space P. Probability flow out of P into its orthogonal complement Q is accounted for by employing the repetitive projection method [12]. Spurious contributions due to "reflections" can be suppressed and backcoupling from Q to P is neglected. This feature has the benefit that, if the calculation has not fully converged, the calculated survival probability and the quantum localization is underestimated.

Figure 2 illustrates the occurrence of quantum localization for a Rydberg atom initially in the $n_i = 50$ level subject to a train of impulses with a scaled frequency $\nu_0 = \nu_T/\nu_{\rm orb} = 2\pi n_i^3/T = 16.8$. Previous calculations at lower frequencies and very small kick strengths indicated that quantum localization could be found [13]. The classical initial conditions in each case correspond to the unperturbed torus shown in Fig. 1 which lies in a chaotic region far from sizable stable islands. After a short period of time, the classical survival probability to be in any bound state for $\Delta p_0 = -0.3$ [Fig. 2(a)] rapidly decays as a function of the number of kicks. Remarkably, the quantum survival probability separates from the classical result after ~30 kicks. The quantum system becomes vastly more stable than the classical system, thereby providing clear evidence of quantum localization. For short times, where the classical evolution mimics the quantum evolution, the survival probability oscillates with a period $\sim 9T$ which provides clues as to the underlying localization mechanism. For $\Delta p > 0$, the survival probability also shows quantum suppression of diffusive ionization but it does not display pronounced oscillations. Instead, the quantum recurrence probability,

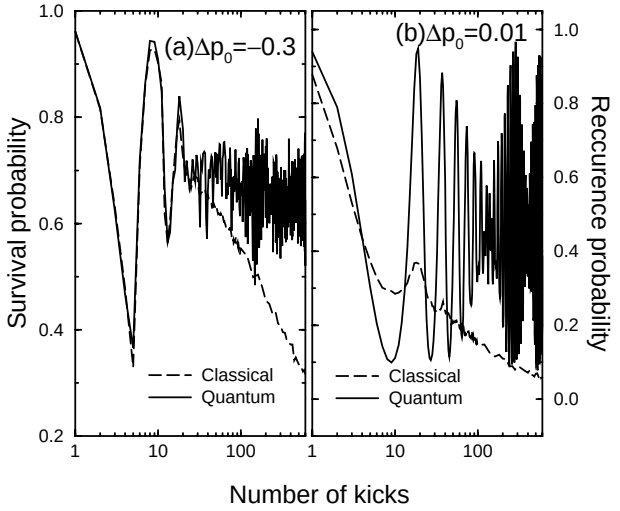

FIG. 2. Survival probability (a) and recurrence probability (b) as a function of the number of kicks for a Rydberg atom initially in the $n_i = 50$ level and for $\nu_0 = 16.8$.

$P_{\rm rec}(t) = |\langle\psi(0)|\psi(t)\rangle|^2$, defined by the probability to return to the initial $n_i = 50$ level exhibits an oscillatory structure [Fig. 2(b)] which is partially mimicked by the classical result.

Signatures of quantum localization are also evident in energy space (Fig. 3). The energy distribution of the evolved quantum state after 600 kicks,

$$|\psi(t = 600T)\rangle = \sum_{n=1}^{N_{\rm max}} c_n(t = 600T)\,|\phi_n^{\rm Stark}\rangle \qquad (6)$$

displays for both $\Delta p_0 = -0.3$ [Fig. 3(a)] and $\Delta p_0 = 0.01$ [Fig. 3(b)] pronounced inhibition of diffusion. In Eq. (6) we have employed a basis of Stark states diagonalizing $H_{\rm Stark}$ [Eq. (4)]. Choosing a Stark basis has the effect of sharpening the observed structures. Two distinct localization mechanisms suppressing energy diffusion can be identified for weak pulses [Fig. 3(b)]: a rapid decay around the central peak and a decaying amplitude of additional peaks. The latter represents quasiresonant excitation into Stark states $|m\rangle$ which are separated from the initial state, $|0\rangle$, by a multiple of the driving frequency, $E_m - E_0 = 2m\pi\nu_T \equiv m\omega$. Suppression of resonant diffusion was analyzed by Jensen *et al.* [9] for a monochromatic microwave field in terms of sequential photoabsorptions with probabilities $P^{\omega}_{m\to m+1}$. This mechanism predicts

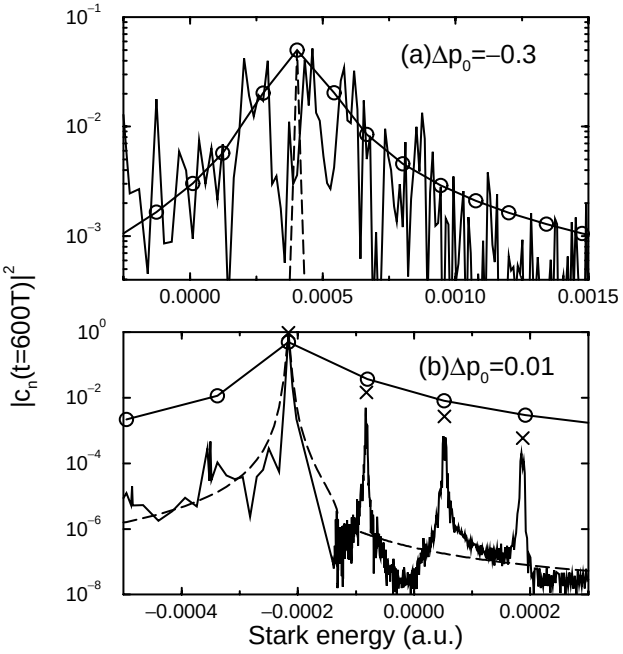

FIG. 3. Stark energy distribution of the final state of the atom after application of 600 kicks with scaled frequency $\nu_0 = 16.8$ and different strengths. Initially, the atom is prepared in the Stark state $|0\rangle$ which has the largest overlap with the $n_i = 50$ hydrogenic level. The crosses are the time-averaged integrated probabilities of the resonant peaks. The solid lines with circles are the average excitation probabilities given by $P^{m\omega}_{0\to m}$ such that the adjacent energy difference between circles is equal to ω. The dashed lines are the dipole coupling strength $|\langle 0|q|\phi_n^{\rm Stark}\rangle|^2$ in arbitrary units.

exponential localization, $P_{0\to m} \propto \exp(-m|\ln P^{\omega}_{0\to 1}|)$. In the kicked atom, the excitation dynamics is fundamentally different due to the equally strong presence of all harmonics. Averaged over the detuning δE_m, direct excitation induced by a single harmonic with frequency $m\omega$ is given by

$$P^{m\omega}_{0\to m} = \frac{|F_{\rm av}\langle m|q|0\rangle|}{\delta E_m}\,\tan^{-1}\left[\frac{\delta E_m}{2|F_{\rm av}\langle m|q|0\rangle|}\right], \qquad (7)$$

where $\langle m|q|0\rangle$ is the dipole coupling from $|0\rangle$ to $|m\rangle$. In the present problem, direct excitation dominates over sequential excitation, $P^{m\omega}_{0\to m} > \prod_{i=0}^{m-1} P^{\omega}_{i\to i+1}$. Consequently, we observe a nonexponential localization in energy space which mimics the energy dependence of the dipole coupling, also displayed in Fig. 3. In fact, the integrated peaks agree quite well with the direct excitation probabilities $P^{m\omega}_{0\to m}$ [Eq. (7)].

For localization to occur, a second localization mechanism must be operative that suppresses nonresonant diffusion, which determines the width of each m-photon peak (including $m = 0$). The width of the dominant peak in Fig. 3(b) agrees with the localization length obtained from the state entropy [14]. By contrast, for $\Delta p_0 = -0.3$ [Fig. 3(a)] the two mechanisms are of comparable strength and a distinction between resonant and nonresonant diffusion is possible only when the evolution of the wave function is analyzed in more detail. We analyze the quantum evolution by expanding the wave function in terms of Floquet states [15] obtained by numerically diagonalizing the period-one evolution operator within the finite Hilbert (P) space. The Floquet quasieigenenergies are complex due to the nonunitary evolution. Components of the wave function that correspond to localized, nondiffusive flow are characterized by vanishing imaginary parts of the quasienergies of the dominant Floquet states. In order to relate the localization to the classical phase space we calculate the Husimi distribution of these localized Floquet states [11,16]. Remarkably, for both $\Delta p_0 = 0.01$ and $\Delta p_0 = -0.3$ the Husimi distributions are localized around unstable fixed points (Fig. 4). The Husimi distribution depicted in Fig. 4(a) is localized at the classical fixed points of a period-$9T$ unstable orbit. Clearly, the Husimi distribution represents a "scar" of the classical unstable periodic orbit [17]. Initially, the electron is near the outer turning point of the orbit at $p_0 \sim 0, q_0 \sim 2$ and acquires a negative momentum. Each kick on the inbound motion speeds up the electron and excites it to a higher energy level including the hydrogenic continuum. Eventually, the electron scatters at the nucleus and acquires a positive momentum. Subsequently, each kick during the outbound part of the trajectory slows down the electron deexciting it to a lower energy level and becoming a bound hydrogenic state once again. Note that three out of nine fixed points lie at positive energies ($H_{\rm at} > 0$) which corresponds to localization in the continuum. The motion along a classical unstable periodic orbit immediately explains the oscillation period ($\sim 9T$) in the survival probability and the

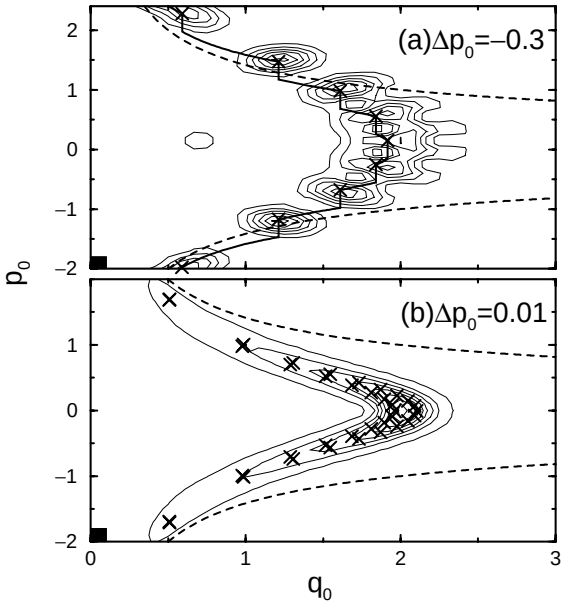

FIG. 4. Contour plot of the Husimi distribution of a quite stable Floquet state for $\nu_0 = 16.8$ (thin solid lines), the classical unstable fixed points (crosses) with period $9T$ (a) and period $17T$ and $19T$ (b). The period $9T$ unstable periodic orbit (thick solid line), and the ionization threshold, $H_{\rm at} = 0$, (thick dashed line) are also depicted. The black squares at the lower left corner correspond to an area of minimum scaled quantum uncertainty $\hbar_0 = 1/n_i = 0.02$. The parameters for the train of pulses are the same as in Fig. 1.

classical-quantum correspondence for short times. The classical phase-space flow proceeds along the unstable orbit for times comparable to the inverse Lyapunov exponent λ^{-1} before it exponentially separates from it at later times. The quantum evolution, on the other hand, localizes along the unstable fixed points.

Similarly, the scarring of the Husimi distribution for $\Delta p_0 = 0.01$ [Fig. 4(b)] is at the root of the oscillations in the recurrence probability with a period $\sim 18T$. In this case, however, the fixed points are distributed very densely in phase space (fixed points with a period $17T$ and $19T$ are plotted in the figure), and quantum mechanics cannot resolve all structures. In scaled units, the uncertainty is given by $\Delta p_0 \Delta q_0 \sim 1/n_i$ and its size by the rectangular area at the lower left corner in Fig. 4. Clearly, more than one fixed point can fit into this area. The absence of oscillations in the survival probability, unlike the recurrence, is also a direct consequence of the fact that unstable periodic orbits exist exclusively among bound states ($H_{\rm at} < 0$) for the positively kicked atom. Once the electron has reached the continuum ($H_{\rm at} > 0$) as it moves away from the nucleus, any additional kicks accelerate the electron further on its outbound journey.

The close connection between the Husimi distributions and the unstable periodic orbits suggests that the quantum localization may be described in terms of the classical dynamics. To this end we consider the total energy excursion along an unstable periodic orbit, $\Delta E = E_{\rm max} - E_{\rm min}$, where and $E_{\rm max}$ and $E_{\rm min}$ are the maximum and minimum Stark energies involved in the periodic orbit. We find ΔE provides a measure of the localization length. For $\Delta p_0 = 0.01$, $\Delta E \approx 6.8 \times 10^{-6}$ a.u., which is smaller than the nearest-neighbor Stark level spacing and is in good agreement with the width of the dominant peak in Fig. 3(b). On the other hand, for $\Delta p_0 = -0.3$, $\Delta E \geq \omega$ is larger than the single-photon spacing. This immediately explains why well-defined multiphoton peaks are absent and the two localization mechanisms merge. Also in this case, ΔE provides an estimate of the width of the energy distribution in Fig. 3(b). Our analysis shows that this relationship holds over a wide parameter range.

In summary, we have demonstrated the existence of quantum localization of the kicked Rydberg atom within a fully chaotic region in phase space and we have shown that it is intimately related to its localization around classical unstable periodic orbits. The localization is not exponential in energy space due to the fact that the high harmonics of the perturbation play a significant role in the excitation dynamics. In order to realize this simplified 1D system experimentally, a quasi-one-dimensional parabolic Rydberg state ($n \sim 400$) has to be prepared as an initial state polarized parallel to the direction of half-cycle pulses. We hope that the present results will stimulate efforts for the experimental realization of quantum localization in the kicked Rydberg atom.

This work was supported by the NSF, by the U.S. DOE OBES, DCS under Contract No. DE-AC05-96OR22646 with LMERC.

[1] F. L. Moore *et al.*, Phys. Rev. Lett. **75**, 4598 (1995).
[2] P. M. Koch *et al.*, Phys. Rep. **255**, 290 (1995).
[3] C. O. Reinhold *et al.*, Phys. Rev. Lett. **79**, 5226 (1997).
[4] M. T. Frey *et al.*, Phys. Rev. A **59**, 1434 (1999).
[5] G. Casati *et al.*, *Lecture Notes in Physics* (Springer, New York, 1979), Vol. 93, p. 334.
[6] P. W. Anderson, Phys. Rev. **109**, 1492 (1958).
[7] S. Fishman *et al.*, Phys. Rev. Lett. **49**, 509 (1982).
[8] G. Casati *et al.*, Phys. Rep. **154**, 77 (1987).
[9] R. V. Jensen *et al.*, Phys. Rep. **201**, 1 (1991).
[10] C. F. Hillermeier *et al.*, Phys. Rev. A **45**, 3486 (1992).
[11] S. Yoshida *et al.*, Phys. Rev. A **59**, R4121 (1999).
[12] S. Yoshida *et al.*, Phys. Rev. A **60**, 1113 (1999).
[13] R. Blümel, in *Classical, Semiclassical and Quantum Dynamics in Atoms*, edited by H. Friedrich *et al. (*Springer, Heidelberg, 1997).
[14] B. Mirbach *et al.*, Ann. Phys. (N.Y.) **265**, 80 (1998).
[15] J. H. Shirley, Phys. Rev. **138**, B979 (1965).
[16] M. Hillery *et al.*, Phys. Rep. **106**, 121 (1984).
[17] E. J. Heller, Phys. Rev. Lett. **53**, 1515 (1984).